

Deriving Complete Constraints in Hidden Variable Models

Michael C. Sachs

Erin E. Gabriel

Robin J. Evans

Arvid Sjölander

5 January 2026

Abstract

Hidden variable graphical models can sometimes imply constraints on the observable distribution that are more complex than simple conditional independence relations. These observable constraints can falsify assumptions of the model that would otherwise be untestable due to the unobserved variables and can be used to constrain estimation procedures to improve statistical efficiency. Knowing the complete set of observable constraints is thus ideal, but this can be difficult to determine in many settings. In models with categorical observed variables and a joint distribution that is completely characterized by linear relations to the unobservable response function variables, we develop a systematic method for deriving the complete set of observable constraints. We illustrate the method in several new settings, including ones that imply both inequality and equality constraints.

1 Introduction

The assumption of a structural model with hidden variables can rule out particular joint distributions both due to observable conditional independence relations, but also more complex

observable conditions, which may not be clear from inspection of the causal model alone. These observable constraints can be used to falsify a structural model in settings where the data contradict these constraints. The instrumental inequalities first discussed in Pearl (1995) for the all binary instrumental variable (IV) setting are the most well-known example of these more complex constraints in the form of inequalities, while the “Verma” constraints (Verma and Pearl, 1991) are a well-known example of observable and thus falsifiable equality constraints representing a more general notion of conditional independence.

In the general IV setting, Bonet (2001) derived inequality constraints showing that, in cases with an IV with more than two categories, there are more observable constraints beyond the binary IV constraint set. Within the specific setting of all discrete observed variables within the classical trivariate IV setting he developed a method for deriving constraints on the observed data distribution implied by the causal assumptions and proved that these are the “sufficient” set of constraints. We will use the term “complete” to refer to what Bonet called sufficient, but the meaning remains the same, i.e. all observable and therefore falsifiable constraints implied by a structural model.

The Bonet (2001) method is what Evans (2012) called the “computationally intensive linear programming technique”. As pointed out by Evans (2012), complete constraints are difficult to derive without using such techniques or algebraic variable elimination algorithms, e.g., Fourier-Motzkin elimination, which become infeasible for moderately sized state spaces. Although other attempts have been made, such as Kang and Tian (2006), the derived constraints are not complete. This is also true for the *nested Markov* characterization which, by construction, only involves equality constraints (Evans and Richardson, 2019; Shpitser et al., 2012; Verma and Pearl, 1991; Richardson et al., 2023); see further in for more details of this.

We conceptually extend the method of Bonet (2001) beyond the IV setting, which due to increased computational power is now feasible in many more settings. We prove that within the class of models that we refer to as “linear”, as defined in Duarte et al. (2023), our method provides the complete set of observable constraints. Linear here refers to settings

with categorical observed variables and a joint distribution that is completely characterized by linear relations to the unobservable response function variables (Balke and Pearl, 1994; Sachs et al., 2023). We also show that for the class of models for which our method provides complete constraints, the fully characterized joint distributions are a subclass of the distributions characterized by the nested Markov model in the same setting. In addition, we show that the proposed method can be used outside the “linear” class to derive at least some of the constraints. We illustrate our method in several examples, providing, to our knowledge, novel constraints. All proofs are in the Appendix and software implementing the method is publicly available on GitHub at <https://github.com/sachsma/meraconstraints>.

2 Notation and Preliminaries

2.1 Notation

Let $\mathcal{G}(\mathbf{W}, \mathbf{U})$ be a hidden variables directed acyclic graph (DAG) representing a nonparametric structural equations model (NPSEM) (Pearl, 2000), over variables $\mathbf{V} = \mathbf{W} \cup \mathbf{U}$ where \mathbf{U} are unobserved and \mathbf{W} are observed. We assume that all variables in \mathbf{W} are discrete and finite, but no assumptions are made about \mathbf{U} . We will write \mathbf{W}_i (or some other index) to denote a subset of \mathbf{W} , and W_i a single element of \mathbf{W} . Let $|\mathbf{W}|$ denote the cardinality of the set \mathbf{W} , and when used for a single variable, for example $|W_i|$, let it denote the number of possible values that variable W_i can take, i.e., the cardinality of its domain. Let $\text{Paobs}(\mathbf{W}_i)$ denote the union of the sets of observed parents of each variable in the set \mathbf{W}_i and $\text{pa}(\mathbf{W}_i)$ denote the union of the sets of all, observed or unobserved, parents of each variable in the set \mathbf{W}_i . Let $\text{Anobs}(\mathbf{W}_i)$ denote the union of the sets of observed ancestors of each variable in \mathbf{W}_i , where, as in Evans and Richardson (2019), W_2 is an ancestor of W_1 if there is a sequence of directed edges $W_2 \rightarrow \dots \rightarrow W_1$, and by definition, we include W_1 itself in the set of ancestors. Let $\text{Chobs}(\mathbf{W}_i)$ be the union of the sets of observed children of variables in \mathbf{W}_i .

2.2 Settings

Our goal is to characterize the distribution $P(\mathbf{W})$, known as the marginal model (because it is marginal with respect to \mathbf{U}), in terms of constraints implied by the NPSEM for (\mathbf{W}, \mathbf{U}) . Following Evans (2016), Section 3.2, we can restrict our attention to a smaller class of hidden variables DAGs that satisfy the following two conditions. In particular, it suffices to consider DAGs where none of the unobserved variables have parents, and where all of the unobserved variables have at least two observed children.

Condition 1 *All unobserved variables are exogenous, i.e., $\text{pa}(U_i) = \emptyset$ for all $U_i \in \mathbf{U}$.*

Condition 2 *The child set of each unobserved variable correspond to a distinct set of observed vertices of at least size 2. That is, for each $U_i \in \mathbf{U}$, $|\text{Chobs}(U_i)| \geq 2$, $\text{Chobs}(U_i) \subseteq \mathbf{W}_i$, and there is no $U_j \in \mathbf{U}$ such that $\text{Chobs}(U_i) \subseteq \text{Chobs}(U_j)$.*

By Lemmas 1–3 of Evans (2016)¹, DAGs where these conditions do not hold can be transformed to DAGs where they do hold without changing the implied marginal model. Briefly, the exogenization process replaces sequences of the form $V_1 \rightarrow U_1 \rightarrow W_1$ by $V_1 \rightarrow W_1$ without changing the marginal model, where V_1 could be observed or unobserved. Following exogenization, any unobserved variable U_1 whose child set is a subset of another unobserved variable U_2 can be absorbed into a common unobserved variable with child set equal to the union of child sets of U_1 and U_2 . Examples of these transformations are given in the Appendix.

Definition 1 *Let $\mathcal{G}(\mathbf{W}, \mathbf{U})$ be a hidden variables DAG that by construction obeys Conditions 1 and 2. Remove all edges that do not originate from variables in \mathbf{U} . The sets of variables in \mathbf{W} that remain connected form a partition of \mathbf{W} called districts. Denote $\mathcal{D}(\mathcal{G}) = \{D_1, \dots, D_k\}$ the set of districts of \mathcal{G} .*

This same concept is called a *c-component* (short for confounded component) by Tian and Pearl (2002b), while the term district is used in, e.g., Richardson (2003), Evans (2018),

¹Here we use the references to the published version of these comments, rather than the arXiv version. The arXiv versions are Lemmas 3.7–3.9.

and Duarte et al. (2023), which we will follow. We further define the c-degree of a district as follows.

Definition 2 Let $\mathcal{G}(\mathbf{W}, \mathbf{U})$ be a hidden variables DAG that follows Conditions 1 and 2. Let D_j be a district in $\mathcal{G}(\mathbf{W}, \mathbf{U})$. The c-degree of D_j is the maximum of 1 and the number of variables U_i in \mathbf{U} for which there exists a $W_k \in D_j$ such that $U_i \in \text{Pa}(W_k)$ in $\mathcal{G}(\mathbf{W}, \mathbf{U})$. The c-degree of $\mathcal{G}(\mathbf{W}, \mathbf{U})$ is the maximum of the c-degrees of its districts.

The example in Figure 1 illustrates the two definitions in this Section. The graph has three districts, two with c-degrees 1 ($\{G\}$, $\{A, C, E\}$) and one with c-degree 2 ($\{B, D, F\}$). Thus, Figure 1 has c-degree 2.

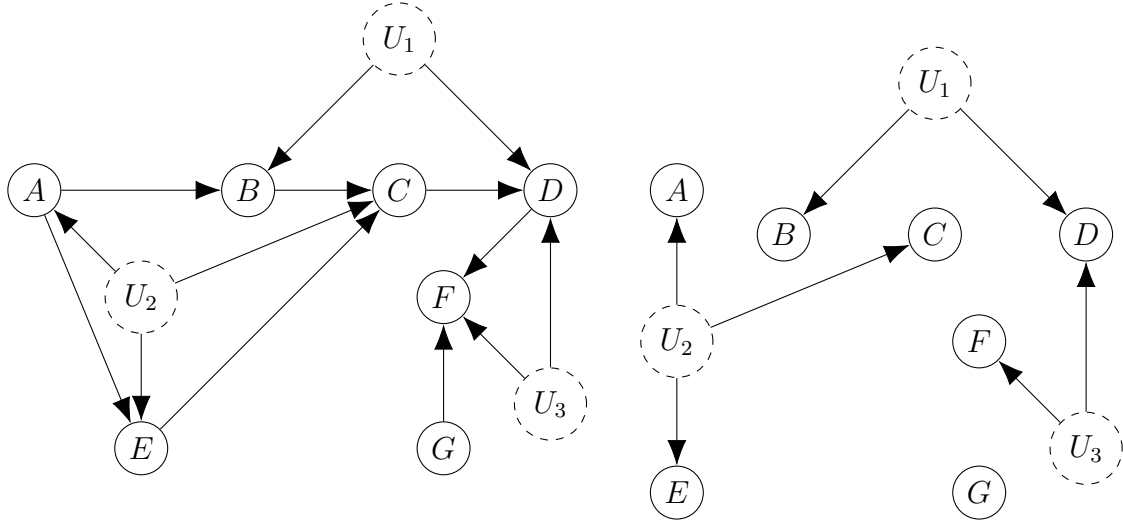


Figure 1: Example to illustrate Definitions 1 and 2. The left figure is the original one, and the right figure has the edges originating from observed variables removed. The graph has three districts: $\{G\}$ and $\{A, C, E\}$ with c-degrees 1 and $\{B, D, F\}$ with c-degree 2.

2.3 Canonical partitioning

A DAG that follows Conditions 1, 2, and that has a c-degree of 1 comprises districts of either singleton observed variables or sets of observed variables that all share a single common unobserved parent. Such DAGs can be transformed into equivalent mixed graphs (containing directed and undirected edges) that remove unobserved variables \mathbf{U} having arbitrary distribution and replaces them with a set of unobserved variables \mathbf{R} that are categorical. These are called *response function variables* by Balke and Pearl (1994) and *selectors* by Bonet (2001). This is possible due to the fact that each observed variable is categorical, which induces a canonical partitioning (Pearl, 2000). See also Theorem 1 of Sachs et al. (2023).

Definition 3 Let $\mathcal{G}(\mathbf{W}, \mathbf{U})$ be a hidden variables DAG that follows Conditions 1, 2, and has a c-degree of 1. The response variable transformation of $\mathcal{G}(\mathbf{W}, \mathbf{U})$ is a mixed graph $\mathcal{G}(\mathbf{W}, \mathbf{R})$ where:

- for each $W_i \in \mathbf{W}$, introduce a new unobserved variable R_{W_i} that is discrete with $|W_i|^{k_i}$ levels, where $k_i = \prod_{V \in \text{Pa}_{\text{obs}}(W_i)} |V|$, and add an edge $R_{W_i} \rightarrow W_i$;
- introduce an undirected edge $R_{W_i} — R_{W_j}$ for every pair of variables W_i, W_j that are in the same district.

The value of R_{W_i} determines the way that W_i responds to its parents. The undirected edges that connect R_{W_i} and R_{W_j} indicate a statistical dependence, so that $P(R_{W_j} = a, R_{W_k} = b) = P(R_{W_j} = a)P(R_{W_k} = b)$ if R_{W_j} and R_{W_k} are not connected by a undirected edge, but $P(R_{W_j} = a, R_{W_k} = b)$ is not necessarily equal to $P(R_{W_j} = a)P(R_{W_k} = b)$ if they are connected. An example is shown in Figure 2. We will refer to R_{W_i} as the response function variable of W_i , and use the notation $\mathbf{R}_{\mathbf{W}_i}$ to denote the vector of response function variables for the vector of observed variables \mathbf{W}_i . It should be noted that response function variables will be connected within a district, but never between different districts.

Remark 1 Let $\mathcal{G}(\mathbf{W}, \mathbf{U})$ be a hidden variables DAG that follows Conditions 1, 2, and has a c-degree of 1. The response variable transformation of $\mathcal{G}(\mathbf{W}, \mathbf{U})$ results in the same structural

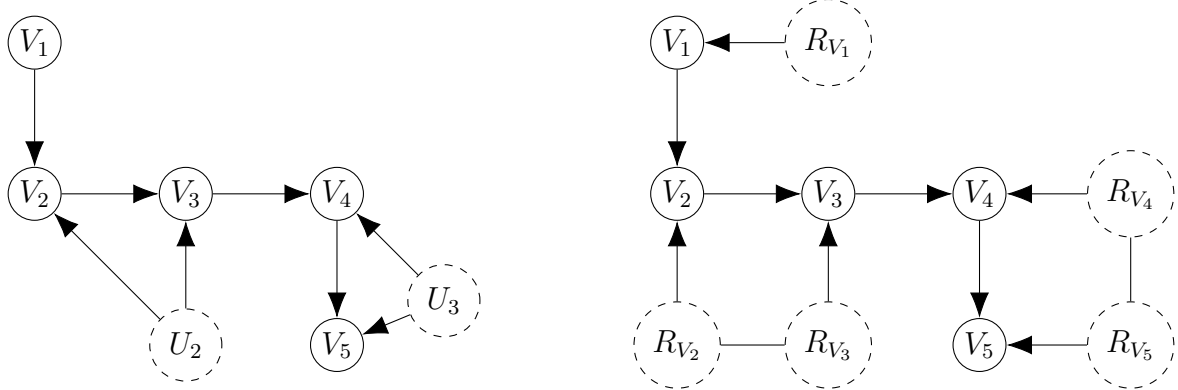


Figure 2: A sequential instrumental variable example, and its response function variable transformation.

model, i.e. results in the same values of all variables under any intervention (including no intervention) on any of the observed variables in the DAG.

The response function variable transformation preserves the marginal model, and also allows us to exploit the discreteness of the observations to formulate a set of linear constraints. Given a value of a response function variable, say $R_{W_i} = b$, there exists a response function $f_{W_i}^b(\text{Paobs}(W_i))$ that determines an observed value for W_i given $\text{Paobs}(W_i)$. So $f_{W_i}^b : \text{domain}(\text{Paobs}(W_i)) \rightarrow \text{domain}(W_i)$. Given values of the response function variables for W_i and all of its ancestors, the value of W_i is determined by recursive substitutions (Sachs et al., 2023; Duarte et al., 2023). Therefore we can write all observable probabilities and interventional probabilities in terms of probabilities of response function variables. Following Tian and Pearl (2002b), we will call the equations relating these two forms of probabilities *functional constraints*.

2.4 Functional constraints

An algorithm and implementation to obtain the set of functional constraints for DAGs that fit a more strict set of criteria than what we consider here was presented in Algorithm 1 of Sachs et al. (2023). A more general algorithm for settings with arbitrary c-degree is presented in Duarte et al. (2023), where the constraints are polynomials. Their Proposition

4 states that the degree of the polynomial constraints is bounded above by the c-degree of the corresponding district. In our next Proposition we explicitly relate the functional constraints to observable probabilities, forming the foundation of the observable constraint derivation.

Proposition 1 *Suppose $\mathcal{G}(\mathbf{W}, \mathbf{U})$ is a hidden variables DAG that follows Conditions 1 and 2. Further, suppose \mathbf{W}_1 is the vector of all variables in the same district D_1 , and let $\mathbf{W}_2 = \text{Paobs}(\mathbf{W}_1) \setminus \mathbf{W}_1$ be the vector of parents of \mathbf{W}_1 that are not part of \mathbf{W}_1 . If D_1 has a c-degree 1, then for all possible values of the vectors $w_1 = (w_{11}, \dots, w_{1k}), w_2 = (w_{21}, \dots, w_{2\ell})$, define the probabilities $P^*(\mathbf{W}_1 = w_1 | \mathbf{W}_2 = w_2)$ as*

$$\prod_{i:W_{1i} \in D_1} P(W_{1i} = w_{1i} | \{\text{Paobs}(\mathbf{W}_1) \cap \text{Anobs}(W_{1i})\} \setminus W_{1i}).$$

Then the functional constraints on $P^(\mathbf{W}_1 = w_1 | \mathbf{W}_2 = w_2)$ under $\mathcal{G}(\mathbf{W}, \mathbf{U})$ are linear functions of response function variable probabilities of $\mathbf{R}_{\mathbf{W}_1}$.*

Let $P(\mathbf{W}_1 = w_1 | \text{do}(\mathbf{W}_2 = w_2))$ denote the joint probability of $\mathbf{W}_1 = w_1$ under the intervention that sets $\mathbf{W}_2 = w_2$. All of the $P^*(\mathbf{W}_1 = w_1 | \mathbf{W}_2 = w_2)$ referenced in Proposition 1 can be given a causal interpretation using the do operator, such that $P^*(\mathbf{W}_1 = w_1 | \mathbf{W}_2 = w_2) = P(\mathbf{W}_1 = w_1 | \text{do}(\mathbf{W}_2 = w_2))$.

Proposition 2 *Suppose $\mathcal{G}(\mathbf{W}, \mathbf{U})$ is a hidden variables DAG that follows Conditions 1, 2, and $\mathbf{W}_1, \mathbf{W}_2$ are as described in Proposition 1. Then all $P(\mathbf{W}_1 = w_1 | \text{do}(\mathbf{W}_2 = w_2))$ are identified and given by $P^*(\mathbf{W}_1 = w_1 | \mathbf{W}_2 = w_2)$.*

We note that, one could also consider similar counterfactual quantities, e.g., $P(\mathbf{W}_1(w_2) = w_1)$, rather than the do-operator interventional quantities and Proposition 2 would also hold.

Consider the example in Figures 3, the left most of which is the classical IV setting. In this case there are 2 districts $\{Z\}$ and $\{X, Y\}$, both with c-degree 1 and Conditions 1 and 2 are satisfied. Letting $\mathbf{W}_1 = \{X, Y\}$ and applying Proposition 1 we have $\mathbf{W}_2 =$

$\text{Paobs}(\{X, Y\}) \setminus \{X, Y\} = \{Z\}$, $\text{Anobs}(Y) = \{X, Z\}$, $\text{Anobs}(X) = \{Z\}$, and

$$\begin{aligned}
\text{P}^*(\mathbf{W}_1 = w_1 | \mathbf{W}_2 = w_2) &= \text{P}(X = x, Y = y | \text{do}(Z = z)) \\
&= \text{P}(Y = y | X = x, Z = z) \text{P}(X = x | Z = z) \\
&= \sum_{b \in \mathcal{B}} \text{P}((R_x, R_y) = b), \text{ for all } x, y, z,
\end{aligned}$$

where $\mathcal{B} = \{(b_x, b_y) : f_Y^{b_y}(f_X^{b_x}(z)) = y \text{ and } f_X^{b_x}(z) = x\}$ for the structural equations $f_Y^{b_y}$ and $f_X^{b_x}$. The series of functional constraints for each combination of values of z, x, y can be represented by the matrix equation

$$\mathbf{p}_{xy \cdot z} = \mathbf{B} \mathbf{r}_{xy},$$

where, for binary X, Y, Z , $\mathbf{p}_{xy \cdot z}$ is the vector of 8 probabilities $[\text{P}(Y = y | X = x, Z = z) \text{P}(X = x | Z = z) : x, y, z \in \{0, 1\}]$, \mathbf{B} is an 8×16 matrix of 0s and 1s, and \mathbf{r}_{xy} is the vector of 16 response function variable probabilities $[\text{P}((R_x, R_y) = (b_x, b_y)) : b_x, b_y \in \{0, 1, 2, 3\}]$.

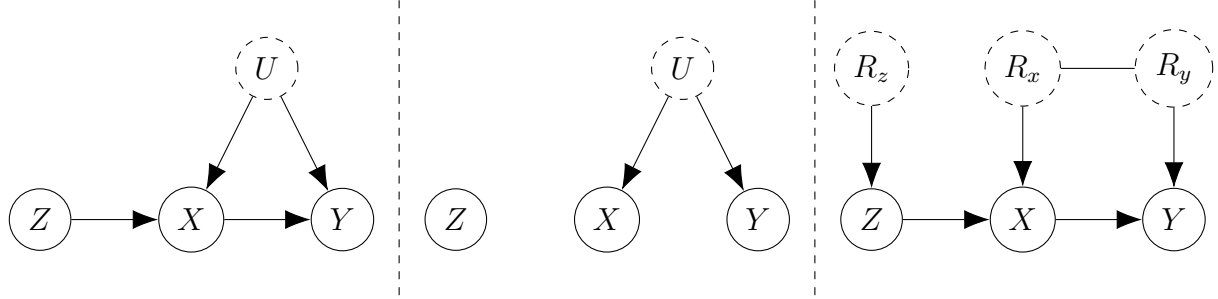


Figure 3: The instrumental variable DAG in original for (left), showing the two districts (center), and response variable form (right).

2.5 Nested Markov models

The nested Markov models (Richardson et al., 2023) further constrain the state-space of these sets of distributions. Briefly put, they allow (generalized) conditional independence constraints to be encoded within a hidden variables DAG model, and in the discrete case to

know that these independences are the only *equality* constraints in the model (Evans, 2018).

While a regular conditional independence relation, for example $X \perp\!\!\!\perp Y \mid Z$, can be expressed as $P(X|Y, Z) = P(X|Z)$, a *nested Markov independence* is a more general statement about a lack of dependence of a quantity on a particular variable. In particular, the quantities in question are probabilities in graphs after removing arrows into certain variables (i.e., intervening on them). For example, they can be expressed as $\sum_B P(D|A, B, C)P(B|A) = g(D, C)$, for some function g ; note the lack of dependence on A here. Such relations are also sometimes called *Verma constraints* after Verma and Pearl (1991), and *post-truncation independences* after Shpitser et al. (2012). Further details are given in the Appendix, Section B.

3 Method for deriving constraints and completeness results

Given those preliminaries, we now detail our algorithm for deriving observable constraints in a hidden variables DAG with discrete and finite observed variables. To summarize briefly, we begin by using d-separation to list all conditional and marginal independencies implied by the DAG, if there are any. Then, for each district, ensuring that the c-degree of each district is 1, we derive the matrix equations representing the linear functional constraints by Proposition 1. These matrix equations describe the extreme points of a convex polyhedron in terms of the unobservable quantities involving probabilities of the response function variables. We can convert this to an equivalent description of the same convex polyhedron in terms of only observable quantities. This is called the vertex-to-halfspace (V-to-H) conversion, and different algorithms exist to efficiently perform this conversion that are implemented in open-source software programs such as `cddlib` (Fukuda, 2018). This is similar to the insight described in Bonet (2001) which was restricted to the instrumental variable setting.

3.1 Description of the algorithm

Inputs: A hidden variables DAG $\mathcal{G}(\mathbf{W}, \mathbf{U})$, that meets Conditions 1, 2, and has c-degree 1.

1. Enumerate the conditional independencies using a standard algorithm based on checking for d-separation, e.g., Van der Zander et al. (2014), or using lines 1–8 of Algorithm 1 of Richardson et al. (2023).

Output: List of standard independence constraints.

2. Identify the set of districts $\mathcal{D} = \{D_1, \dots, D_k\}$.
3. Do the response function variable transformation of \mathcal{G} into \mathcal{G}^\dagger as described in Section 2.3.
4. For each district D_j :
 - (a) Derive the formula for $P^*(\mathbf{W}_1 = w_1 | \mathbf{W}_2 = w_2)$, where \mathbf{W}_1 are all the observed variables in D_j and $\mathbf{W}_2 = \text{Paobs}(\mathbf{W}_1) \setminus \mathbf{W}_1$, using Proposition 1.
 - (b) For each combination of w_1, w_2 , derive the functional probabilities, i.e.,

$$\sum_{b \in \mathcal{B}} P(\mathbf{R}_{\mathbf{W}_1} = b),$$

where \mathcal{B} is the set of response function variable values that are compatible with the observation vector w_1, w_2 .

- (c) Construct the matrix representing the system of linear equations relating

$$P^*(\mathbf{W}_1 = w_1 | \mathbf{W}_2 = w_2) = \sum_{b \in \mathcal{B}} P(\mathbf{R}_{\mathbf{W}_1} = b) \Leftrightarrow \mathbf{p} = \mathbf{B}\mathbf{r}.$$

- (d) Add a row of all 1s to \mathbf{B} which represents the constraint that the response function variable probabilities all sum to 1.

(e) Convert $\mathbf{p} = \mathbf{Br}$ to the H-representation, e.g., using the double description method (Fukuda, 2018; Motzkin et al., 1953).

Output: The H-representation and the vector \mathbf{p} of the formulae for $P^*(\mathbf{W}_1 = w_1 | \mathbf{W}_2 = w_2)$ for each district

The H-representation consists of two rational matrices H_i, H_e and rational vectors b_i, b_e such that

$$H_i \mathbf{p} \leq b_i \text{ and } H_e \mathbf{p} = b_e.$$

In other words, it provides a representation of inequality and equality constraints in terms of the observable probability vector. Continuing with the instrumental variable example, the second district which contains X and Y yields the matrix \mathbf{B}

$$\begin{pmatrix} 1 & 1 & 1 & 1 & 0 & 0 & 0 & 0 & 0 & 0 & 0 & 0 & 0 & 0 & 0 & 0 & 0 \\ 0 & 0 & 0 & 0 & 1 & 1 & 1 & 1 & 0 & 0 & 0 & 0 & 0 & 0 & 0 & 0 & 0 \\ 0 & 0 & 0 & 0 & 0 & 0 & 0 & 0 & 0 & 1 & 1 & 1 & 1 & 0 & 0 & 0 & 0 \\ 0 & 0 & 0 & 0 & 0 & 0 & 0 & 0 & 0 & 0 & 0 & 0 & 0 & 1 & 1 & 1 & 1 \\ 1 & 0 & 1 & 0 & 1 & 0 & 0 & 0 & 0 & 0 & 0 & 0 & 0 & 1 & 0 & 0 & 0 \\ 0 & 1 & 0 & 0 & 0 & 1 & 0 & 1 & 0 & 1 & 0 & 0 & 0 & 0 & 0 & 0 & 0 \\ 0 & 0 & 0 & 0 & 0 & 0 & 1 & 0 & 1 & 0 & 1 & 0 & 0 & 0 & 1 & 0 & 0 \\ 0 & 0 & 0 & 1 & 0 & 0 & 0 & 0 & 0 & 0 & 0 & 0 & 0 & 1 & 0 & 1 & 0 \end{pmatrix}$$

where the rows correspond to the constraints on the vector of probabilities $[P(Y = y | X =$

$x, Z = z) \mathbf{P}(X = x | Z = z)$ for

$$(x, y, z) = \begin{pmatrix} 0 & 0 & 0 \\ 1 & 0 & 0 \\ 0 & 1 & 0 \\ 1 & 1 & 0 \\ 0 & 0 & 1 \\ 1 & 0 & 1 \\ 0 & 1 & 1 \\ 1 & 1 & 1 \end{pmatrix}.$$

After adding the row of 1s to the \mathbf{B} matrix and doing the V-to-H conversion, we obtain the H-representation defined by $b_i = (0, 0, 0, 0, 1, 1, 0, 1, 0, 1, 0, 0)^\top$,

$$H_i = \begin{pmatrix} 0 & 0 & 0 & 0 & -1 & 0 & 0 & 0 \\ -1 & -1 & -1 & 0 & 0 & 1 & 0 & 0 \\ 0 & 1 & 0 & 0 & -1 & -1 & -1 & 0 \\ -1 & 0 & 0 & 0 & 0 & 0 & 0 & 0 \\ 0 & 0 & 1 & 0 & 1 & 0 & 0 & 0 \\ 1 & 0 & 0 & 0 & 0 & 0 & 1 & 0 \\ 0 & 0 & 0 & 0 & 0 & -1 & 0 & 0 \\ 0 & 0 & 0 & 0 & 1 & 1 & 1 & 0 \\ 0 & -1 & 0 & 0 & 0 & 0 & 0 & 0 \\ 1 & 1 & 1 & 0 & 0 & 0 & 0 & 0 \\ 0 & 0 & -1 & 0 & 0 & 0 & 0 & 0 \\ 0 & 0 & 0 & 0 & 0 & 0 & -1 & 0 \end{pmatrix},$$

$b_e = (-1, -1)^\top$, and

$$H_e = \begin{pmatrix} -1 & -1 & -1 & -1 & 0 & 0 & 0 & 0 \\ 0 & 0 & 0 & 0 & -1 & -1 & -1 & -1 \end{pmatrix}.$$

These expressions encode both inequality and equality constraints. For example, the 5th row of H_i and corresponding element of b_i encode the constraint

$$P(Y = 1, X = 0|Z = 0) + P(Y = 0, X = 0|Z = 1) \leq 1,$$

which is one of the classic instrumental inequalities as derived by Pearl (1995). The equality constraints encoded by H_e are simply the standard probabilistic constraints:

$$\sum_{x,y \in \{0,1\}} P(Y = x, X = y|Z = z) = 1, \text{ for } z = 0, 1. \quad (1)$$

3.2 Completeness results

Proposition 3 *Let \mathcal{G} be a DAG satisfying Conditions 1, 2, and having c-degree 1. Then the constraints derived from the algorithm combined with any conditional independencies are complete.*

In other words, if every district in a DAG has at most one latent common cause, then the constraints derived by our algorithm are necessary and sufficient, i.e., there are no other observable constraints implied by the structural assumptions. This result stems from the linearity of the functional constraints, which means that we can then use standard results from computational geometry convert them to observable constraints. The fact that the V- and H- representations are equivalent ensures nothing is lost from the V-to-H conversion which is the cornerstone of our approach to getting the observable constraints. The district factorization of the marginal distribution and our Proposition 1 ensures that there are no components of the marginal distribution left unexamined.

As a negative example, consider the DAG in Figure 8, left side, often referred to as the

triangle scenario. The triangle scenario has c-degree 3, and comprises a single district. Our algorithm cannot be applied in this case, however, it is known that some observed probability distributions are incompatible with the triangle scenario. For example, Wolfe et al. (2019) demonstrates that the distribution where $P(A = 1, B = 1, C = 1) = P(A = 0, B = 0, C = 0) = 1/2$ is incompatible with the triangle scenario. An additional example is the left side of Figure 7. As discussed in Section 5 and 6, one can modify such graphs to obtain some or all constraints in some settings.

3.3 Identifying nontrivial constraints

Definition 4 *An observable constraint is **nontrivial** if it restricts the full joint distribution beyond the standard probabilistic constraints (i.e., probabilities sum to 1 and are between 0 and 1).*

An example of an observable constraint is $P(W_1 = w_1) \geq 0$, which is trivial because it is implied by the axioms of probability and not the structural model. Another example is given in Equation (1) in the illustration of our algorithm on the IV setting. We propose a simple procedure for identifying the subset of potentially nontrivial constraints from the output of our algorithm. It is based on the observation that the H-representations are linear constraints on a vector of probabilities, i.e.,

$$H_i \mathbf{p} \leq b_i \text{ and } H_e \mathbf{p} = b_e,$$

where $\mathbf{p} = [P^*(\mathbf{W}_1 = w_1 | \mathbf{W}_2 = w_2) : \text{ for all possible values of } w_1, w_2]$. The unconstrained space of probabilities is the cross product of the probability simplices of the appropriate dimension, which is a convex polyhedron. Since the constraints are linear in these probabilities, violations can be witnessed at the extreme points of the unconstrained polyhedron. If these extreme points do not produce violations, the constraints are definitely trivial. Thus, our approach is to enumerate the extreme points of the unconstrained polyhedron, and then test if any of the derived constraints are ever violated at these points; violations identify

potentially nontrivial constraints. We state this in the following proposition and illustrate it in the IV example.

Proposition 4 *Suppose $\mathcal{G}(\mathbf{W}, \mathbf{U})$ is a hidden variables DAG that follows Conditions 1, 2, with the H-representation of constraints on a given district from Algorithm 3.1 of the form*

$$H_i \mathbf{p} \leq b_i \text{ and } H_e \mathbf{p} = b_e,$$

where $\mathbf{p} = [P^*(\mathbf{W}_1 = w_1 | \mathbf{W}_2 = w_2) : \text{ for all possible values of } w_1, w_2]$. Let $\check{\mathbf{P}}$ denote the cross-product of probability simplices, one for each unique value of w_2 , in the order corresponding to \mathbf{p} . Any nontrivial constraints encoded by H_i and H_e are violated by at least one of the extreme points of $\check{\mathbf{P}}$.

Continuing with the IV example from the previous section and applying Proposition 4, the $\check{\mathbf{P}}$ space is the cross-product of 2 probability simplices, one for $z = 0$ and one for $z = 1$. The extreme points are represented in the following matrix, where each row represents an instance of the vector

$$\begin{aligned} & [P^*(0, 0|0), P^*(1, 0|0), P^*(0, 1|0), P^*(1, 1|0), \\ & P^*(0, 0|1), P^*(1, 0|1), P^*(0, 1|1), P^*(1, 1|1)] \end{aligned}$$

$$\begin{pmatrix} 1 & 0 & 0 & 0 & 1 & 0 & 0 & 0 \\ 0 & 1 & 0 & 0 & 1 & 0 & 0 & 0 \\ 0 & 0 & 1 & 0 & 1 & 0 & 0 & 0 \\ 0 & 0 & 0 & 1 & 1 & 0 & 0 & 0 \\ 1 & 0 & 0 & 0 & 0 & 1 & 0 & 0 \\ 0 & 1 & 0 & 0 & 0 & 1 & 0 & 0 \\ 0 & 0 & 1 & 0 & 0 & 1 & 0 & 0 \\ 0 & 0 & 0 & 1 & 0 & 1 & 0 & 0 \\ 1 & 0 & 0 & 0 & 0 & 0 & 1 & 0 \\ 0 & 1 & 0 & 0 & 0 & 0 & 1 & 0 \\ 0 & 0 & 1 & 0 & 0 & 0 & 1 & 0 \\ 0 & 0 & 0 & 1 & 0 & 0 & 1 & 0 \\ 1 & 0 & 0 & 0 & 0 & 0 & 0 & 1 \\ 0 & 1 & 0 & 0 & 0 & 0 & 0 & 1 \\ 0 & 0 & 1 & 0 & 0 & 0 & 0 & 1 \\ 0 & 0 & 0 & 1 & 0 & 0 & 0 & 1 \end{pmatrix}.$$

We then check whether $H_i \tilde{\mathbf{p}} > b_i$ or $H_e \tilde{\mathbf{p}} \neq b_e$ for each $\tilde{\mathbf{p}}$ in the rows of the above matrix.

We find that the equality constraints are never violated, and the 2nd, 3rd, 5th and 6th rows of H_i are violated by at least one of the extreme points. These constraints are (after some simple algebra) the classical instrumental inequalities:

$$P(Y = 1, X = 1|Z = 0) + P(Y = 0, X = 1|Z = 1) \leq 1$$

$$P(Y = 0, X = 1|Z = 0) + P(Y = 1, X = 1|Z = 1) \leq 1$$

$$P(Y = 1, X = 0|Z = 0) + P(Y = 0, X = 0|Z = 1) \leq 1$$

$$P(Y = 0, X = 0|Z = 0) + P(Y = 1, X = 0|Z = 1) \leq 1.$$

We can do the similar procedure for the other district which contains the singleton Z . However, singleton districts with no parents cannot give any nontrivial constraints, so we omit the details.

We note that the algorithm identifies all nontrivial observable constraints, but we do not claim that it identifies only such constraints. We provide an example below using the front door graph, Figure 4, which is known to have no observable nontrivial constraints.

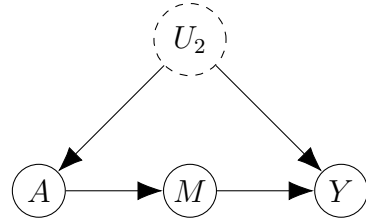


Figure 4: Front door model.

When applying our algorithm to the front door model in Figure 4, we get the following constraints reported as potentially nontrivial:

$$-P(A = 0) + P(A = 0)P(Y = 0|A = 0, M = 1) \leq 0$$

$$P(A = 0) + P(A = 1)P(Y = 0|A = 1, M = 1) \leq 1$$

$$P(A = 0) - P(A = 0) = 0$$

$$-P(A = 0) - P(A = 1) = -1.$$

These have been simplified from the original form they were provided by the algorithm to allow them to fit easily on the page and clearly illustrate that they are trivial. The reason these are flagged as nontrivial is clear when written in terms of the interventional quantities

that were tested by the algorithm:

$$\begin{aligned}
& - P(A = 0, Y = 0 \mid \text{do}(M = 0)) - P(A = 0, Y = 1 \mid \text{do}(M = 0)) \\
& + P(A = 0, Y = 0 \mid \text{do}(M = 1)) \leq 0 \\
& P(A = 0, Y = 0 \mid \text{do}(M = 0)) + P(A = 0, Y = 1 \mid \text{do}(M = 0)) \\
& + P(A = 1, Y = 0 \mid \text{do}(M = 1)) \leq 1 \\
& P(A = 0, Y = 0 \mid \text{do}(M = 0)) + P(A = 0, Y = 1 \mid \text{do}(M = 0)) \\
& - P(A = 0, Y = 0 \mid \text{do}(M = 1)) - P(A = 0, Y = 1 \mid \text{do}(M = 1)) = 0 \\
& - P(A = 0, Y = 0 \mid \text{do}(M = 0)) - P(A = 0, Y = 1 \mid \text{do}(M = 0)) \\
& - P(A = 1, Y = 0 \mid \text{do}(M = 1)) - P(A = 1, Y = 1 \mid \text{do}(M = 1)) = -1.
\end{aligned}$$

If one were able run an experiment to intervene on M directly, such that they interventional quantities would be identified directly by conditional factual quantities, these would be non-trivial constraints. However, translating them to the identifying functionals under the front door model, we obtain trivial constraints on any observed distribution. Thus, constraints flagged by the algorithm as potentially nontrivial should be always be investigated manually whenever possible. However, enforcing or testing all flagged constraints is not incorrect as trivial constraints does not impose restrictions on the distribution. The tripartite Bell example in Subsection 4.3 illustrates a situation where it would be cumbersome to manually investigate all potentially nontrivial constraints.

4 Novel Examples

4.1 Sequential instrumental variables

The model for this example is shown in Figure 2. This DAG satisfies Conditions 1, 2, and it has a c-degree of 1. There are three districts: $\{V_1\}, \{V_2, V_3\}, \{V_4, V_5\}$. Using standard

d-separation criteria, we find the conditional independence relations $(V_1, V_2) \perp\!\!\!\perp (V_4, V_5) | V_3$. Applying our Algorithm and then Proposition 4, we find the nontrivial constraints below that are recognizable as two sets of the instrumental inequalities, one for each of the two districts with unobserved variables:

$$P(V_2 = 1, V_3 = 1 | V_1 = 0) + P(V_2 = 1, V_3 = 0 | V_1 = 1) \leq 1$$

$$P(V_2 = 1, V_3 = 0 | V_1 = 0) + P(V_2 = 1, V_3 = 1 | V_1 = 1) \leq 1$$

$$P(V_2 = 0, V_3 = 1 | V_1 = 0) + P(V_2 = 0, V_3 = 0 | V_1 = 1) \leq 1$$

$$P(V_2 = 0, V_3 = 0 | V_1 = 0) + P(V_2 = 0, V_3 = 1 | V_1 = 1) \leq 1$$

$$P(V_4 = 1, V_5 = 1 | V_3 = 0) + P(V_4 = 1, V_5 = 0 | V_3 = 1) \leq 1$$

$$P(V_4 = 1, V_5 = 0 | V_3 = 0) + P(V_4 = 1, V_5 = 1 | V_3 = 1) \leq 1$$

$$P(V_4 = 0, V_5 = 1 | V_3 = 0) + P(V_4 = 0, V_5 = 0 | V_3 = 1) \leq 1$$

$$P(V_4 = 0, V_5 = 0 | V_3 = 0) + P(V_4 = 0, V_5 = 1 | V_3 = 1) \leq 1.$$

4.2 Nested equivalent models with distinct inequalities

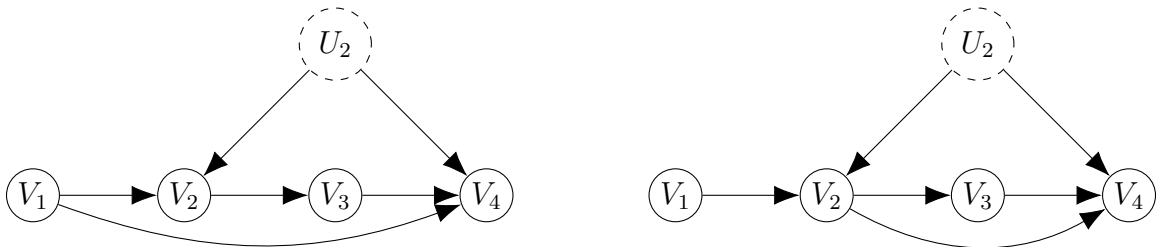


Figure 5: Two graphs that are nested Markov equivalent, but which have distinct inequality constraints.

Figure 5 shows an example of two graphs that are nested Markov equivalent, but which differ when inequalities are also considered. Both graphs satisfy Conditions 1, 2, have c-degree 1, and they both have three districts: $\{V_1\}$, $\{V_2, V_4\}$, $\{V_3\}$. Both graphs imply that $V_1 \perp\!\!\!\perp V_3 | V_2$. In both graphs, the districts $\{V_1\}$ and $\{V_3\}$ imply only trivial constraints. The

interesting constraints are associated with the district $\{V_2, V_4\}$, and probabilities of the form

$$\begin{aligned} P^*(V_2 = v_2, V_4 = v_4 | V_1 = v_1, V_3 = v_3) = \\ P(V_2 = v_2 | V_1 = v_1)P(V_4 = v_4 | V_2 = v_2, V_1 = v_1, V_3 = v_3). \end{aligned}$$

The graph on the left does not have any nontrivial constraints aside from the conditional independence (though our Algorithm flags some as potentially nontrivial similar to the front door model). Note that the graph on the right is such that after intervening on V_3 we obtain an instrumental variables model over V_1, V_2, V_4 (for each level of V_3). In contrast, the graph on the left is saturated over that margin. Therefore, we get some nontrivial inequality constraints in the right graph that are not present under the left graph. They are

$$\begin{aligned} P^*(V_2 = 0, V_4 = 1 | V_1 = 0, V_3 = 0) + P^*(V_2 = 0, V_4 = 0 | V_1 = 1, V_3 = 0) \leq 1 \\ P^*(V_2 = 0, V_4 = 0 | V_1 = 0, V_3 = 0) + P^*(V_2 = 0, V_4 = 1 | V_1 = 1, V_3 = 0) \leq 1 \\ P^*(V_2 = 1, V_4 = 0 | V_1 = 0, V_3 = 0) + P^*(V_2 = 1, V_4 = 1 | V_1 = 1, V_3 = 0) \leq 1 \\ P^*(V_2 = 1, V_4 = 1 | V_1 = 0, V_3 = 0) + P^*(V_2 = 1, V_4 = 0 | V_1 = 1, V_3 = 0) \leq 1 \\ P^*(V_2 = 0 | V_1 = 1, V_3 = 0) + P^*(V_2 = 0, V_4 = 0 | V_1 = 0, V_3 = 1) \\ -P^*(V_2 = 0, V_4 = 0 | V_1 = 1, V_3 = 1) \leq 1 \\ P^*(V_2 = 0 | V_1 = 0, V_3 = 0) + P^*(V_2 = 0, V_4 = 0 | V_1 = 1, V_3 = 1) \\ -P^*(V_2 = 0, V_4 = 0 | V_1 = 0, V_3 = 1) \leq 1 \\ P^*(V_2 = 1 | V_1 = 1, V_3 = 0) + P^*(V_2 = 1, V_4 = 0 | V_1 = 0, V_3 = 1) \\ -P^*(V_2 = 1, V_4 = 0 | V_1 = 1, V_3 = 1) \leq 1 \\ P^*(V_2 = 1 | V_1 = 0, V_3 = 0) + P^*(V_2 = 1, V_4 = 0 | V_1 = 1, V_3 = 1) \\ -P^*(V_2 = 1, V_4 = 0 | V_1 = 0, V_3 = 1) \leq 1. \end{aligned}$$

Here we are writing the constraints in terms of the *star* probabilities, which are equal to observable probabilities, because in this case they are more concise and make it easier to

relate them to nested Markov constraints.

4.3 Tripartite Bell graphs

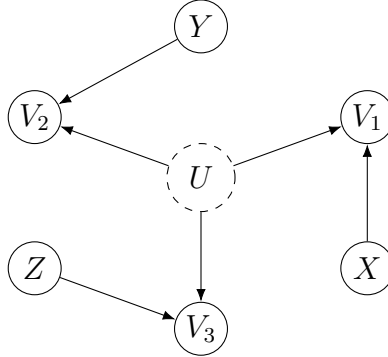


Figure 6: The tripartite Bell scenario.

Figure 6 is a well-known causal model in quantum physics. An incomplete set of constraints has been derived using the entropy method in Gläßle et al. (2018). Our algorithm finds the complete set of constraints in this setting in less than 0.5 CPU-hours on a laptop running Ubuntu 22 with an AMD Ryzen 7 and 32 GB of RAM. First we identify the standard independencies $X \perp\!\!\!\perp (V_2, V_3, Y, Z)$, $Y \perp\!\!\!\perp (V_1, V_3, X, Y)$, and $Z \perp\!\!\!\perp (V_1, V_2, X, Y)$. The subsequent part of the algorithm yields an additional 53,894 constraints total, out of which there are 53,856 inequality constraints, in agreement with Śliwa (2003) and Pironio et al. (2011). Our method further identifies 32,866 of those as potentially nontrivial constraints, 6 of which are equality constraints. The 6 equality constraints repeat the independence relations $(V_1, V_3) \perp\!\!\!\perp Y$, $(V_1, V_2) \perp\!\!\!\perp Z$, and $(V_2, V_3) \perp\!\!\!\perp X$. An example of one of the inequality constraints, using the notation $P(v_1 v_2 v_3 | xyz) = P(V_1 = v_1, V_2 = v_2, V_3 = v_3 | X = x, Y = y, Z = z)$, is

$$\begin{aligned}
& P(001|010) + P(010|101) - P(110|001) - P(010|100) - \\
& P(000|111) - P(001|000) - P(011|000) \leq 0.
\end{aligned}$$

5 Extension to potentially incomplete linear constraints

We extend our Algorithm to allow for DAGs with c-degree greater than 1. Prior to applying the algorithm in 3.1:

1. check that $|D_j| \geq 2$, otherwise pass through;
2. create a new unobserved variable U_j^* ;
3. if there exists an edge from any unobserved variable to W_i in D_j , add an edge $U_j^* \rightarrow W_i$;
4. then remove every unobserved variable other than U_j^* from D_j .

Remark 2 *Let \mathcal{G}' be a DAG satisfying Conditions 1, 2, and with c-degree greater than 1. Let \mathcal{G} be the causal model obtained from \mathcal{G}' by merging unobserved variables so that the c-degree is 1. Then the constraints emitted by \mathcal{G} hold under \mathcal{G}' .*

We now consider the two examples for which our algorithm did not apply as discussed in Section 3.2. Figure 7, left side, shows an example DAG that also appears in Duarte et al. (2023). This DAG has two districts, $\{V_1, V_3, V_6\}$ that has c-degree 1 and $\{V_2, V_4, V_5\}$ that has c-degree 2. It satisfies Conditions 1 and 2, but since the c-degree is greater than 1, we cannot guarantee that the constraints derived by our algorithm are complete. In this case, we proceed by merging the unobserved variables U_1 and U_3 into a single unobserved variable U_{13} that has child set equal to the union of the child sets of U_1 and U_3 (Figure 7, right side). This makes the potentially nonlinear problem into a linear one. The constraints we obtain in these cases are still valid, but they are not necessarily complete.

In this example, we find 8 nontrivial constraints for the first district, 4 inequality and 4 equality constraints. The equality constraints are again strictly nested Markov independences that state $P^*(V_1 = v_1, V_6 = v_6 | V_2 = v_2) = P^*(V_1 = v_1 | V_2 = v_2)$, while the inequality constraints take the form

$$P^*(V_1 = 0, V_3 = 0, V_6 = 0 | V_2 = 1) \leq P^*(V_1 = 0, V_6 = 0 | V_2 = 0),$$

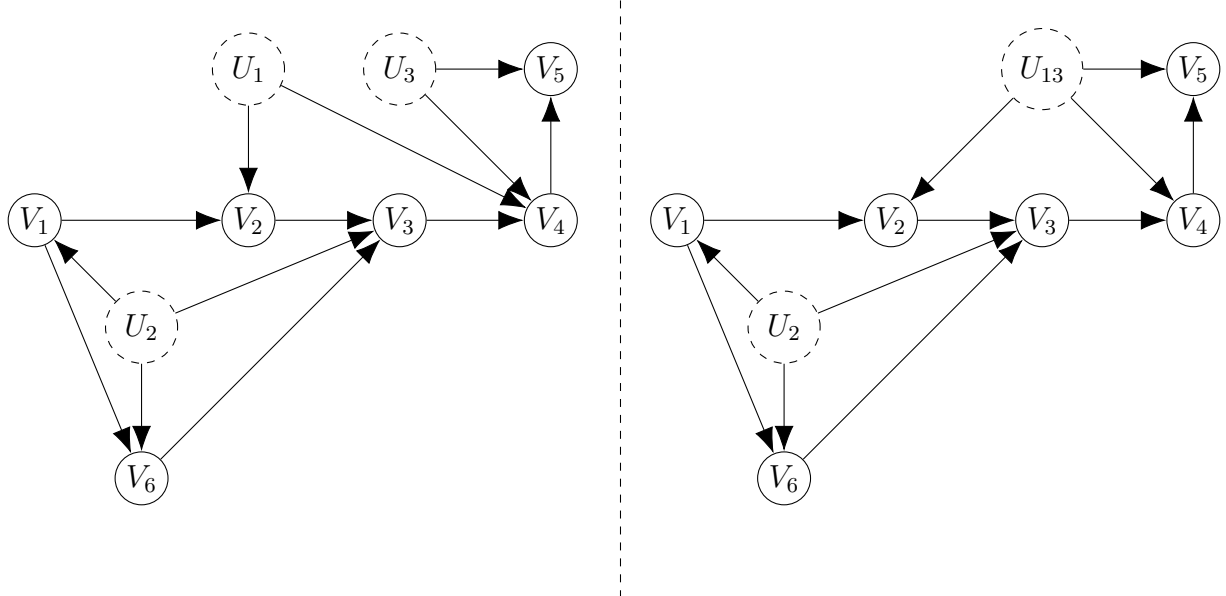


Figure 7: Example model with two districts and c-degree 2 (left side), and the model after merging the unobserved variables U_1 and U_3 to make the c-degree 1 (right side).

for different levels of V_1, V_3, V_6 .

After merging U_1 and U_3 in the second district and applying our Algorithm, we find 1118 potentially nontrivial constraints. In the interest of space, we do not reproduce them here, but given an observed distribution, it is straightforward to check whether they are violated or not using the matrix representations of the constraints.

This process of merging latent variables to create a DAG with c-degree 1 can be applied as a pre-processing step before using our Algorithm to obtain some constraints in more general settings, but again this does not necessarily yield the complete constraints. In words, for models that have more than one unobserved variable in at least one district, the constraints obtained by our Algorithm are necessary but not necessarily complete. That is, they must hold but there may be more constraints than the linear ones we are able to derive.

We now consider the Triangle scenario. If we merge the three unobserved variables into a single common parent of all three observable variables, which is depicted in the right side of Figure 8, we can apply our algorithm. Our algorithm in this case does not produce any nontrivial constraints that can witness incompatibility. In this case, we know that this set of

constraints is incomplete, because of those presented in Wolfe et al. (2019).

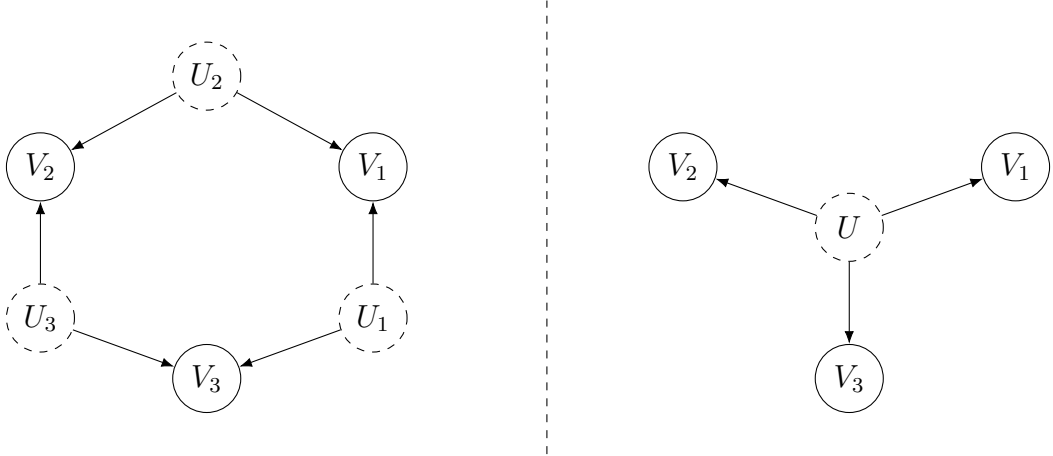


Figure 8: The triangle scenario (left) and the graph obtained by merging the three unobserved variables into one.

6 Observationally equivalent DAGs

Multiple graphs may be observationally equivalent and therefore emit the same set of constraints. For example, the graph $X \rightarrow Y$ is observationally equivalent to the graph where X and Y share an unobserved parent. Proposition 5 of Evans (2016) and its extensions (Ansanelli, 2022) can be used to obtain graphs with lower c-degree that are observationally equivalent to graphs with c-degree greater than one. We note that this may not be causal, but it is *observationally* equivalent to the DAG under study. Proposition 5 of Evans (2016), adapted to our notation, provides a recipe for converting between observationally equivalent DAGs that may have different c-degrees.

Proposition 5 *Let \mathcal{G} be a DAG that meets Conditions 1 and 2, and \mathbf{C}, \mathbf{D} be disjoint sets of observed vertices. If*

- $\mathbf{C} \cup \mathbf{D} = \text{Chobs}(U_i)$, i.e., they comprise a district;
- $c \notin \text{Chobs}(U_j)$ for all $c \in \mathbf{C}$, for any other unobserved vertex $U_j \neq U_i$;

- $\text{pa}(\mathbf{C}) \subseteq \text{pa}(d)$ for every $d \in \mathbf{D}$;

then the graph obtained by replacing every path of the form $c \leftarrow U_i \rightarrow d$ with $c \rightarrow d$ for every pair $c \in \mathbf{C}$, $d \in \mathbf{D}$ has the same constraints as \mathcal{G} .

The Henson-Lal-Pusey Henson et al. (2014) result provides conditions under which one can add an edge to a DAG without changing the constraints.

Proposition 6 (HLP Proposition) *Let \mathcal{G} be a DAG that meets Conditions 1 and 2, and W_1 and W_2 observed nodes. If:*

- $\text{pa}(W_1) \subseteq \text{pa}(W_2)$;
- if $W_1 \subseteq \text{Chobs}(U_1)$ for some U_1 unobserved, then $W_2 \subseteq \text{Chobs}(U_1)$;

then the graph has the same constraints as the one in which, in addition, we have the edge $W_1 \rightarrow W_2$.

Combining the HLP proposition with the following result from Ansanelli (2022) (adapted to our notation) can show observational equivalences in cases where Proposition 5 cannot, and also subsumes it. We include Proposition 5 because it may be easier to recognize situations where it can be applied, in some cases.

Proposition 7 (Strong Face Splitting) *Let \mathcal{G} be a DAG meeting Conditions 1 and 2, containing the following unobserved vertices U_1, \dots, U_k that share $D = \bigcap_{i=1}^k \text{Chobs}(U_i)$. Let $C_i = \text{Chobs}(U_i) \setminus D$. If the following conditions hold:*

- $\text{pa}(C_i) \cup C_i \subseteq \text{pa}(d)$ for each $d \in D$, for $i = 1, \dots, k$;
- if for an unobserved vertex U_j , we have $c \in \text{Chobs}(U_j)$ for some $c \in \bigcup_{i=1}^k C_i$ then $D \subseteq \text{Chobs}(U_j)$;

then the DAG obtained from the observed subgraph of \mathcal{G} , adding the unobserved vertices $U_1^*, \dots, U_k^*, U_{k+1}^*$ and corresponding edges $\{U_1^* \rightarrow c : c \in C_1\}, \dots, \{U_k^* \rightarrow c : c \in C_k\}, \{U_{k+1}^* \rightarrow d : d \in D\}$ has the same constraints as \mathcal{G} .

A simple example of using these results is shown in Figure 9. The three DAGs are known to be observationally equivalent, but our method applies only to the rightmost DAG because it has c-degree one. Thus our method can provide complete constraints in settings with c-degree greater than one, for any DAG that can be converted via Proposition 5 or Propositions 6 and 7 to a DAG with c-degree one.

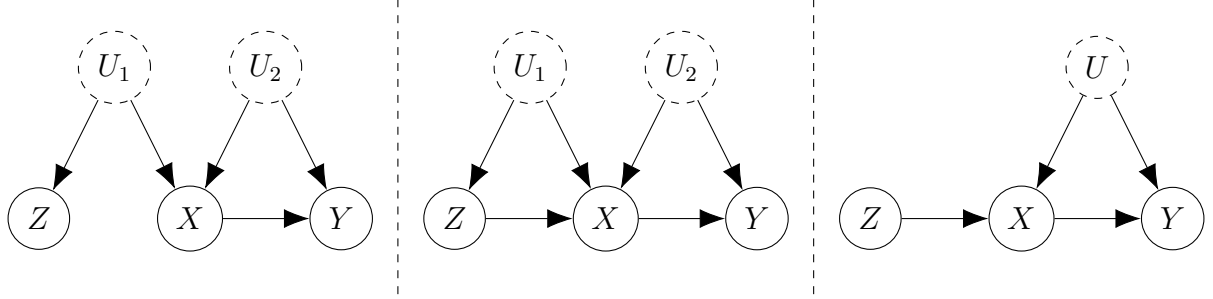


Figure 9: A DAG with c-degree two (left). Applying the HLP Proposition, we get the center DAG that has equivalent constraints. Applying Strong Face Splitting to the center DAG, we get the observationally equivalent classic IV DAG on the right that has c-degree one. Equivalently, we can apply Proposition 5 to the left and center DAGs with $\mathbf{C} = \{Z\}$ and $\mathbf{D} = \{X\}$.

The example in Figure 10 illustrates two graphs that Proposition 7 can be used to show the equivalence of, but Proposition 5 cannot. The original DAG has a single district with c-degree two. Applying the Strong Face Splitting result in combination with the HLP Proposition, we obtain an observationally equivalent DAG with two districts, one with c-degree one and one with c-degree two. Proposition 5 or Strong Face Splitting in combination with the HLP Proposition could once again be applied to the resulting graph to further reduce the c-degree. This is merely to demonstrate that there are settings where Strong Face Splitting in addition to the HLP Proposition can show equivalence where Proposition 5 cannot.

In the case of Figure 7, we cannot apply either of these Propositions to reduce the c-degree. Consider the district containing $\{V_2, V_4, V_5\}$ that has c-degree two. In order to reduce the c-degree by removing U_1 , we would need $V_2 \in \mathbf{C}$. Since V_1 is a parent of V_2 but not of V_4 nor V_5 , the first condition of Proposition 5 cannot be satisfied. We also cannot remove U_3 or U_1 using Strong Face Splitting because the parent set of V_4 does not contain the parents of V_2 ,

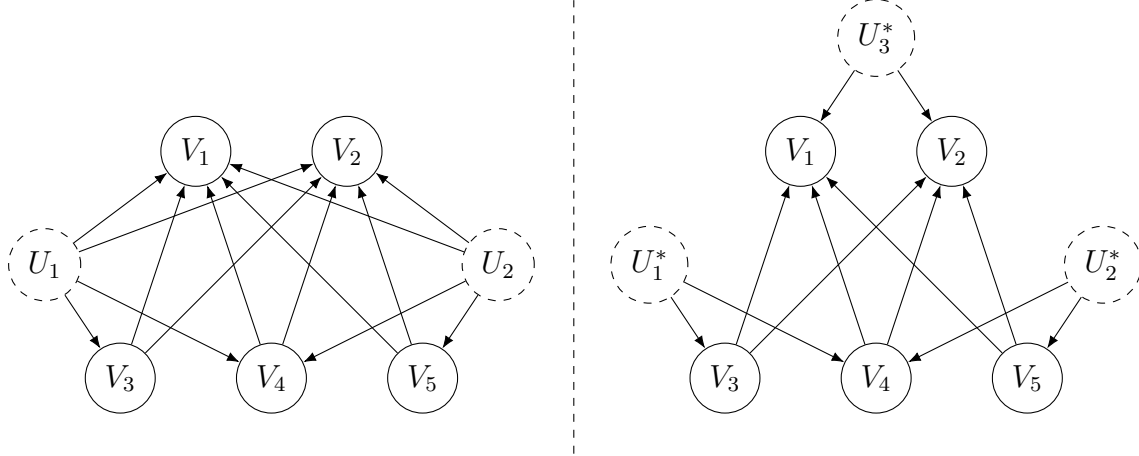


Figure 10: An example DAG (left) where Proposition 7 can be applied to show observational equivalence of the two DAGs, but not Proposition 5.

and V_2 is not a parent of V_4 .

7 Conclusion

Bonet (2001) observed that the complete set of observable constraints in the instrumental variables model can be derived with tools from computational geometry. We have extended this observation to a much broader class of causal models with unobserved variables, showing that a similar set of tools can be used to derive the complete set of equality and inequality constraints for any graph of c-degree one. Several of our examples illustrate that this method includes nontrivial equality constraints, similar to the Verma constraints or nested Markov constraints. However, unlike those sets of constraints, our derived set of constraints may also include inequality constraints. To distinguish this class of constraints from the previous equality-only nested Markov ones, we suggest the name MERA constraints, particularly when the set of constraints contain both equalities and inequalities and are complete.

The method is limited to DAGs with finite and discrete observed variables, though no assumptions are made about the state space of the unobserved variables. The method of deriving the constraints can be computationally demanding, as the number of facets of the polytope grows superexponentially in the number of variables. The precise complexity of

the algorithm depends on the connectivity of the DAG, and the method can be computationally simple in graphs with many variables if they reside in different districts with simple connections between district. It may be possible to adapt multithreaded implementations of computational geometry algorithms to perform this task (Bruns et al.), or to extend the pruning approach of (Shridharan and Iyengar, 2023) to this setting to reduce the size of the linear program in certain cases. However, once derived for a given DAG, they are symbolic expressions that can be applied to any dataset or distribution.

This method has potential applications in causal discovery with hidden variables, as this provides a finer stratification of causal models into equivalence classes than does independence testing or equality constraints alone. How to most effectively incorporate these constraints in causal discovery algorithms is an open question. These constraints also have potential applications in constrained statistical inference and partial identification.

References

M. M. Ansanelli. Observational equivalence between causal structures. Master’s thesis, Instituto de Fisca Teórica, 2022.

A. Balke and J. Pearl. Counterfactual probabilities: Computational methods, bounds and applications. In *Uncertainty in artificial intelligence*, pages 46–54. Elsevier, 1994.

B. Bonet. Instrumentality tests revisited. In *Proceedings of the Seventeenth conference on Uncertainty in Artificial Intelligence*, pages 48–55, 2001.

W. Bruns, B. Ichim, C. Söger, and U. von der Ohe. Normaliz algorithms for rational cones and affine monoids. Available at <https://www.normaliz.uni-osnabrueck.de>.

G. Duarte, N. Finkelstein, D. Knox, J. Mummolo, and I. Shpitser. An automated approach to causal inference in discrete settings. *Journal of the American Statistical Association*, pages 1–16, 2023.

R. J. Evans. Graphical methods for inequality constraints in marginalized DAGs. In *2012 IEEE International Workshop on Machine Learning for Signal Processing*, pages 1–6. IEEE, 2012.

R. J. Evans. Graphs for margins of Bayesian networks. *Scandinavian Journal of Statistics*, 43(3):625–648, 2016.

R. J. Evans. Margins of discrete Bayesian networks. *The Annals of Statistics*, 46(6A):2623 – 2656, 2018. doi: 10.1214/17-AOS1631. URL <https://doi.org/10.1214/17-AOS1631>.

R. J. Evans and T. S. Richardson. Smooth, identifiable supermodels of discrete DAG models with latent variables. *Bernoulli*, 25(2):848 – 876, 2019. doi: 10.3150/17-BEJ1005. URL <https://doi.org/10.3150/17-BEJ1005>.

K. Fukuda. *cdd, cddplus and cddlib homepage*. Swiss Federal Institute of Technology, Zurich., 2018. URL https://people.inf.ethz.ch/fukudak/cdd_home/.

T. Gläßle, D. Gross, and R. Chaves. Computational tools for solving a marginal problem with applications in Bell non-locality and causal modeling. *Journal of Physics A Mathematical General*, 51(48):484002, Nov. 2018. doi: 10.1088/1751-8121/aae754.

J. Henson, R. Lal, and M. F. Pusey. Theory-independent limits on correlations from generalized bayesian networks. *New Journal of Physics*, 16(11):113043, 2014.

C. Kang and J. Tian. Inequality constraints in causal models with hidden variables. In *Proceedings of the Twenty-Second Conference on Uncertainty in Artificial Intelligence*, pages 233–240, 2006.

T. Motzkin, H. Raiffa, G. Thompson, and R. Thrall. The double description method. *Contributions to Theory of Games*, 2, 1953.

J. Pearl. On the testability of causal models with latent and instrumental variables. In

Proceedings of the Eleventh conference on Uncertainty in artificial intelligence, pages 435–443, 1995.

J. Pearl. *Causality*. Cambridge University Press, New York, 2000.

S. Pironio, J.-D. Bancal, and V. Scarani. Extremal correlations of the tripartite no-signaling polytope. *Journal of Physics A: Mathematical and Theoretical*, 44(6):065303, jan 2011. doi: 10.1088/1751-8113/44/6/065303. URL <https://doi.org/10.1088/1751-8113/44/6/065303>.

T. Richardson. Markov properties for acyclic directed mixed graphs. *Scandinavian Journal of Statistics*, 30(1):145–157, 2003.

T. S. Richardson, R. J. Evans, J. M. Robins, and I. Shpitser. Nested Markov properties for acyclic directed mixed graphs. *The Annals of Statistics*, 51(1):334–361, 2023.

M. C. Sachs, G. Jonzon, A. Sjölander, and E. E. Gabriel. A general method for deriving tight symbolic bounds on causal effects. *Journal of Computational and Graphical Statistics*, 32(2):567–576, 2023.

I. Shpitser, T. S. Richardson, J. M. Robins, and R. Evans. Parameter and structure learning in nested Markov models. In *28th Conference on Uncertainty in Artificial Intelligence (Causal Structure Learning Workshop)*, 2012.

M. Shridharan and G. Iyengar. Scalable computation of causal bounds. *Journal of Machine Learning Research*, 24(237):1–35, 2023. URL <http://jmlr.org/papers/v24/22-1081.html>.

J. Tian and J. Pearl. A general identification condition for causal effects. In *Aaai/iaai*, pages 567–573, 2002a.

J. Tian and J. Pearl. On the testable implications of causal models with hidden variables.

In *Proceedings of the Eighteenth conference on Uncertainty in artificial intelligence*, pages 519–527, 2002b.

B. Van der Zander, M. Liskiewicz, and J. Textor. Constructing separators and adjustment sets in ancestral graphs. In *CI@ UAI*, pages 11–24, 2014.

T. Verma and J. Pearl. Equivalence and synthesis of causal models. *Computer Science Department Technical Report, UCLA*, page R150, 1991.

E. Wolfe, R. W. Spekkens, and T. Fritz. The inflation technique for causal inference with latent variables. *Journal of Causal Inference*, 7(2), July 2019. ISSN 2193-3677. doi: 10.1515/jci-2017-0020. URL <http://dx.doi.org/10.1515/jci-2017-0020>.

C. Śliwa. Symmetries of the Bell correlation inequalities. *Physics Letters A*, 317(3-4):165–168, 2003. doi: 10.1016/S0375-9601(03)01115-0.

A Examples of transformations that do not change the marginal model

The examples in the following Figures are adapted from Figures 4 and 5 from Evans (2016).

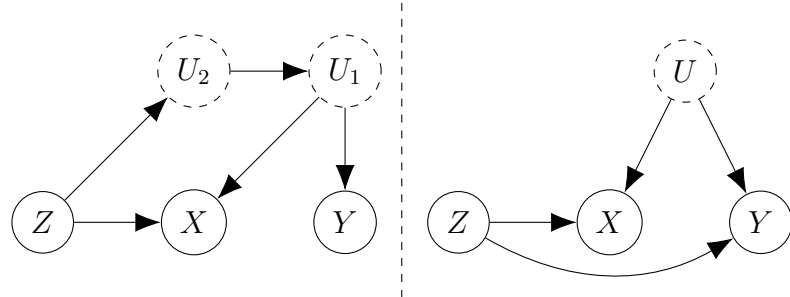


Figure 11: An example of the exogenization process. The two graphs induce the same marginal model over $\{Z, X, Y\}$. The graph on the right side satisfies Condition 1, but the graph on the left does not.

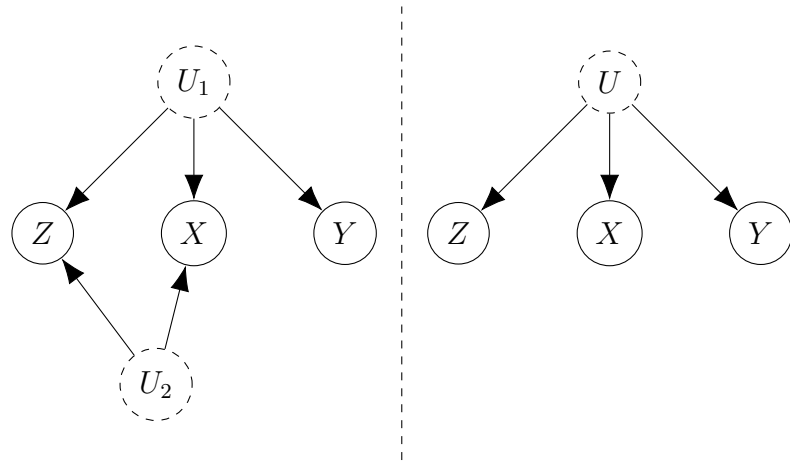


Figure 12: An example of the “nested unobserved variable absorbing” process. The two graphs induce the same marginal model over $\{Z, X, Y\}$. The graph on the right side satisfies Condition 2, but the graph on the left does not.

B Nested Markov model

Here we give a more elaborate discussion of the nested Markov model.

We sort into an arbitrary topological ordering with all unobserved variables first; this we can do since these can, without loss of generality, always be assumed to be parentless and disjoint. Now taking the first of the observed variables, we ‘glue’ it onto each of its unobserved parents.

For subsequent observed variables, we take the district, the observed parents, and the observed parents of the district, as its *Markov blanket*. This gives us

$$W_k \perp\!\!\!\perp \mathbf{W}_? \setminus \{\text{Paobs}(W_k) \cup \text{Disobs}(W_k)\} \mid \text{Paobs}(W_k) \cup \text{Disobs}(W_k) \setminus \{W_k\}. \quad (2)$$

Further, this action can remove certain edges into $\mathbf{W}_?$. That is, it will remove any edges *into* $\mathbf{W}_?$ (i.e., via $W_i \rightarrow W_j$) that are not connected by latent variables to W_k .

C Proofs

Proof of Proposition 1

This follows from Lemma 1 of Tian and Pearl (2002a), with different notation which requires the substitution of their Q_j with $Q_j = P^*(\mathbf{W}_1 = w_1 | \mathbf{W}_2 = w_2)$ and $T_i = \mathbf{W}_1$. Proposition 3 of Duarte et al. (2023) states that the functional constraints on these probabilities depend only on the unobserved variable within the district, and by their Proposition 4, they are linear. This covers part 2. See also Lemma 2 of Tian and Pearl (2002b).

Proof of Proposition 2

This follows directly from Lemma 1, part (i) of Tian and Pearl (2002a) and the definition of *Causal Effect Identification* in Pearl (2000) Definition 3.2.4, page 77.

Proof of Proposition 3

The district factorization allows us to recover the joint observable distribution $P(\mathbf{W})$ from the joints within each district, say \mathbf{p}_m then we can focus on the districts individually. See Equation 27 and Lemma 1 of Tian and Pearl (2002a). Our derivation of the functional constraints uses this district factorization, and under the assumption of c-degree 1, no further factorization of the functional constraints can be done into polynomial constraints. Thus the functional constraint equations are V-representations of a convex polyhedra in the probability space. The H-representation is equivalent for the same polyhedron, i.e., it represents the same constraints. Thus all functional constraints are enumerated and preserved by the V-to-H conversion. As the functional constraints only involve the unobserved variables within the district, the only cross-district constraints are conditional independences, which are enumerated as a separate step.

Proof of Proposition 4

The constraints are linear transformations of the interventional probabilities. It is an H-representation of a convex polytope \mathbf{P} , say, which is contained in the convex polytope of the model that has only the probabilistic constraints, say $\check{\mathbf{P}}$. Each row of the H-representation is minimized or maximized at one of the extreme points of $\check{\mathbf{P}}$. Thus at least one of the extreme points of the unconstrained model would violate the causal constraints, if they are possible to violate. This is by the fundamental theorem of linear programming.

Proof of Remark 2

From Duarte et al. (2023), the constraints in the c-degree greater than 1 case are polynomials. Linear constraints can be derived from those polynomials by combining products into new variables, and those linear constraints hold in the polynomial model by a simple change of variables.